J Appl Electrochem (2008) 38:1275–1283
DOI 10.1007/s10800-008-9553-z

ORIGINAL PAPER

Stability of the electrodeposition process for CoPt alloy formation

O. Berkh · Y. Shacham-Diamand · E. Gileadi

Received: 10 December 2007 / Revised: 3 March 2008 / Accepted: 18 March 2008 / Published online: 4 April 2008

Abstract The stability of the process for electrodeposition of CoPt alloys from ammonium citrate electrolytes containing $[Pt(NO_2)_2(NH_3)_2]^0$ as the source of Pt was studied. Voltammetric monitoring of the anodic oxidation of the electrolyte and deposition of CoPt on the cathode showed the effect of the changes of the nature of the Pt complex on the performance of the plating bath. Anodic oxidation of the Pt complex was shown to involve mainly the oxidation of NO_2^- and to some extent NH_3 ligands. The cathodic process is accompanied by reduction of free NO_2^-. The reduction of this anion in the bound form is highly inhibited. In contrast, its oxidation at the anode proceeds almost as readily in the bound form as that in the free form.

Keywords CoPt alloys · Magnetic alloys · Alloy deposition · Bath stability · Metal-films

1 Introduction

A stable process for electrodeposition of hard magnetic alloys is of great importance for manufacturing of magnetic micro-electromechanical systems (MEMS) and magnetic recording elements [1, 2]. Among several possible electrodeposited alloys, CoPt alloys are the most promising, as annealed equiatomic alloys possess very high magnetic parameters [3–5]. Furthermore, as-deposited CoPtP alloys exhibit magnetic properties acceptable for some applications [6–19] where high temperature annealing is forbidden or limited. These CoPt and CoPtP alloys can be deposited with current efficiencies and deposition rates up to 20% and 12 μm/h, respectively, from citrate electrolytes containing $[Pt(NO_2)_2(NH_3)_2]^0$ as the source of Pt.

Intensive exploration of the electrodeposited CoPt and CoPtP alloy films for application in magnetic discs started more than a decade ago [6]. During the following years, the films were studied mainly in terms of their thickness, structure and magnetic properties. The importance of epitaxial growth, substrate material and its structure for the deposition of films with high magnetic parameters was shown by Zangari, Cavallotti et al. [7–18]. The results of these investigations pointed to the great potential of electrodeposition for manufacturing CoPt and CoPtP permanent magnet films. Nevertheless, no industrial application of this process has yet been reported.

The main problem encountered with the CoPt and CoPtP deposition processes is the so-called total-charge effect [19]. It was observed that the current efficiency (CE) and the characteristics of the CoPt film formed by electrodeposition change with total charge passed through the electrolyte in previous runs. It has been suggested that partial decomposition of the $[Pt(NO_2)_2(NH_3)_2]^0$ complex led to this behavior. Replacement of some or all the ligands in the Pt(II) complexes by water was shown to be responsible for the increase of CE in the deposition of platinum by itself [20–24].

The electrodeposition of Pt from its tetra-chloro-comlex $[PtCl_4]^{2-}$ has been practised for about a century, for the preparation of platinized platinum electrodes as reversible hydrogen reference electrodes. A review of electroplating of Pt on base metals was given in 1988 [25]. A new plating bath, employing the tetrammine complex $[Pt(NH_3)_4]^{2+}$ as

O. Berkh · Y. Shacham-Diamand
Department of Physical Electronics, School of Engineering, Tel Aviv University, Ramat Aviv 69978, Israel

E. Gileadi (✉)
School of Chemistry, Faculty of Exact Sciences, Tel Aviv University, Ramat Aviv 69978, Israel
e-mail: gileadi@post.tau.ac.il

the source of Pt, in a phosphate buffer at pH 10.0–10.6 (referred to as the "Q-salt" bath) was developed at Johnson Matthey Corp. [26]. This bath was studied in detail in a series of papers by Pletcher et al. [20–24]. Other baths, employing $[Pt(NO_2)_2(NH_3)_2]^0$ (the so-called "P-bath") and even the aqua-complex $[Pt(H_2O)_4]^{2+}$, which is fairly stable in strong acidic solutions, were considered. An interesting alternative bath that has been suggested [27] is that containing $[Pt(NO_2)_2SO_4]^{2-}$, or its analog using sulfamate instead of sulfate as the ligand. A review discussing the plating of the platinum-group metals was published recently [28].

Considering the high positive standard potential for deposition of divalent platinum, ($E^0 = +1.118$ V vs. SHE), it should be easy to electroplate this metal with high CE (similar to silver, for example). This is not the case, however, since the aqua-complex of Pt is generally unstable, and a suitable complexing agent is required. The choice of the ligand is difficult, since it should have two properties that are inherently contradictory. On the one hand, the resulting complex should be thermodynamically stable in the solution, ensuring long-term stability and good reproducibility of the performance of the bath. On the other hand, the kinetics of the equilibrium between the complex and the free ion in solution should be fast, allowing satisfactory deposition rate. The tetrammine complex operating at high pH (the "Q-bath") seemed to satisfy this requirement only at temperatures very close to the boiling point of water, making it rather difficult to operate the bath. Pletcher et al. [20–24] found that the performance of the bath is improved if it is treated first, to replace at least two of the NH_3 ligands by water. Similar behavior was found also for other complexes of platinum, such as the tetranitrito and the diammine-dinitrito-platinum (II) complexes.

When electroplating of an alloy such as CoPt is considered, the above problems may be further complicated by the need to consider the stability and complexing properties of the alloying elements as well. Thus, the aqua-complex $[Pt(H_2O)_4]^{2+}$ may be a good source for Pt when plated by itself. However, since it is stable only in strong acid, it cannot be used to form the CoPt alloy, which might corrode in this medium. Similarly, the tetrammine complex $[Pt(NH_3)_4]^{2+}$, which can yield a good plating bath in phosphate buffer at pH 10.0–10.6, may not be suitable, since another complexing agent (such as citrate) would have to be added to keep the Co^{2+} ions in solution. As the $[Pt(NO_2)_2(NH_3)_2]^0$ complex can be used in mild alkaline or mild acid solutions, it seems to be the most suitable for preparation of CoPt plating baths. This complex together with citrate is used by most investigators. However, adding citrate could change the nature of the Pt-containing complex, possibly replacing its ligands.

In order to develop a stable electrolyte, it is necessary to understand the way by which the total charge passed changes the chemical properties of the electrolyte and, hence, the quality of the plated film. In the current work, the changes in the behavior of citrate electrolyte for CoPt deposition during long operation were studied by cyclic voltammetry (CV) and linear sweep voltammetry (LSV). These changes are possibly associated with the decomposition of the $[Pt(NO_2)_2(NH_3)_2]^0$ complex or replacement of some of its ligands during electrolysis. The effects of anodic oxidation and cathodic reduction of the Pt complex on the stability of the CoPt deposition process were shown. Process stability was found to be improved by pre-oxidation of the electrolyte in the anodic compartment of the cell and using it subsequently as the catholyte.

2 Experimental

Deposition of the films was conducted at pH 8 at 50 °C, from electrolytes containing 0.1 M $(NH_4)_3$ Cit, 50 mM $CoSO_4$ and 10 mM $[Pt(NO_2)_2(NH_3)_2]^0$. The electrolyte was stirred with a magnetic stirrer and plating was conducted in both one- and two-compartment cells. Two-compartment cells allowed good isolation between the anolyte and the catholyte and separation of the effects associated with the electrochemical processes occurring at the anode and the cathode. Deposition in two-compartment cells was carried out from as-prepared and pre-oxidized electrolytes. The deposition was conducted on Cu foils in a 50 ml baths. A Pt gauze (200 mesh) with an area of 12 cm^2 was used as the anode. The cathodic current density was 30 mA cm^{-2} (total current 15 mA).

The CE of CoPt alloy deposition was calculated using the data on film composition and the added weight of the sample following deposition. The Co and Pt contents in the film were determined by EDS analysis using JSM-6300 Scanning Electron Microscope, equipped with Oxford Energy Dispersive Spectrometer.

For the cyclic and LSV experiments, an ECO CHEMIE μAutolab electrochemical instrument was used. The working platinum disc electrode was polished before each scan with Buehler polishing cloth and suspensions of alumina powders, particle size 0.3 μm. The electrode area in these experiments was 0.031 cm^2. All potentials were measured with respect to saturated calomel electrode (SCE). The potential limits of CV were from +0.15 to −1.2 V and from +0.15 to +1.7 V in the cathodic and anodic regions, respectively. The scan rate was 100 mV s^{-1}. LSV measurements were taken from −0.4 to −1.2 V, while the disc electrode was rotated at 500 rpm and the potential was scanned at 1 mV s^{-1}.

3 Results

3.1 Total charge effect

The effect of total charge on CE and Pt concentration in the deposits is shown in Fig. 1. The thickness of the films deposited was in the range 1–10 μm. When deposition is conducted from an as-prepared electrolyte in one- and two-compartment cells, the initial CE is close to zero. It increases gradually during operation, leveling off when the total charge passed exceeds about 2 Ah dm^{-3}. This amount of charge is equivalent to the formation of some (yet unidentified) species, at a concentration of about 0.04 mol dm^{-3} (assuming $n = 2$). In deposition from a pre-oxidized electrolyte, the CE starts at about 6% and increased gradually, leveling off faster, at a total charge of 0.7 Ah dm^{-3}, and reaching values close to those found for the as-prepared electrolyte, following long electrolysis.

Similar phenomena were observed earlier for the electrolyte containing 100 mM $CoSO_4$ [19]. The maximal values of CE observed for the electrolytes with 50 mM $CoSO_4$ were 8–10%, while those for electrolyte with 100 mM $CoSO_4$ were 18–20%. The initial Pt content in the deposits was about 35–37 at % (vs. 20–25 at % in the case of 100 mM $CoSO_4$), tending to decrease with total charge passed. This indicates that the increase of CE observed with doubling the concentration of $CoSO_4$ in solution is caused mainly by an increase in the partial current density for Co deposition, with little or no effect on the rate of Pt deposition.

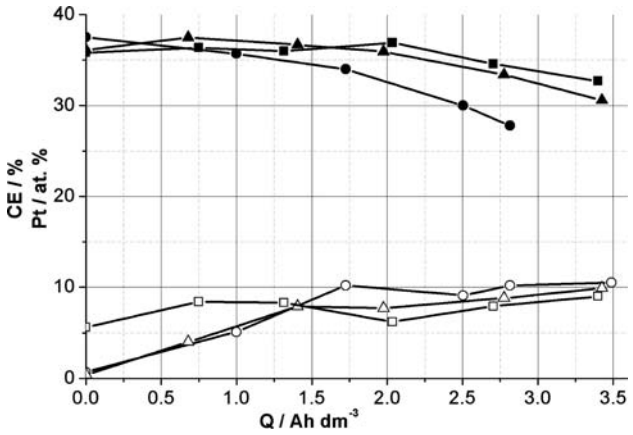

Fig. 1 The effect of total charge on current efficiency of CoPt alloy deposition (CE) and on the Pt concentration in the film. Deposition was conducted at pH 8, 50 °C and at 30 mA cm^{-2}, from electrolytes containing 0.1 M $(NH_4)_3$ Cit, 50 mM $CoSO_4$ and 10 mM $[Pt(NO_2)_2(NH_3)_2]^0$. ●—Pt; ○—CE Deposition in one-compartment cell from as-prepared electrolyte, ▲—Pt; △—CE Deposition in two-compartment cell from as-prepared electrolyte, ■—Pt; □—CE Deposition in two-compartment cell from the electrolyte after preliminary oxidation in the anodic compartment at a potential of +1.2 V, and at 25 °C. The total charge passed in the anodic oxidation is 1.7 Ah dm^{-3}

3.2 Monitoring the electrolytes by voltammetry

The results of monitoring the behavior of the electrolytes during long operation in one- and two-compartment cells are shown in Figs. 2–4.

3.2.1 Characterization of as-prepared electrolyte

The CV in the cathodic region in an as-prepared electrolyte (0.0 Ah dm^{-3}, Fig. 2a), showed a small wave starting at about −0.6 V tending to form a plateau in the range of −(0.65–0.75) V (see inset for more details), followed by a high wave rising at −(0.75–0.7) V.

The LSV is characterized by a small wave starting to rise also at about −0.6 V, followed by a high wave starting at potentials negative to the reversible potential for hydrogen evolution at pH = 8 (−0.72 V vs. SCE). Since in this system the CE for deposition of both metals is only 1–2%, the observed polarization current must be associated mainly with hydrogen evolution (0.0 Ah dm^{-3}, Fig. 2b).

The CV in the anodic region exhibits a wide wave with a peak near +0.9 V SCE. The height of the peak is about 12.5 mA cm^{-2}, as seen in Fig. 2c (for 0.0 Ah dm^{-3}). This wave is associated with the presence of the $[Pt(NO_2)_2\ (NH_3)_2]^0$ complex, since no such peak was observed in its absence.

The CV observed in the anodic region could be the result of superposition of several processes: oxidation of the $[Pt(NO_2)_2\ (NH_3\ )_2]^0$ complex, of ammonia and of citrate. It was shown in the literature [29] that the anodic oxidation of ammonia and citrate are both highly accelerated in the presence of Co^{2+}. Part of the current observed in this region may also be due to oxygen evolution, since the reversible potential for this process is +0.51 V, SCE at pH = 8.

3.2.2 Effect of total charge for operation in one-compartment cell

In the CV conducted in the cathodic region, the small wave rising at about −0.6 V decreased with total charge passed and almost disappeared when it exceeds 1.4 Ah dm^{-3}. Although the general shape of the large wave did not change significantly, noticeable polarization was observed. This effect increased with the total charge passed and after 2.8 Ah dm^{-3} reached about 100 mV as seen in Fig. 2a.

The changes in the cathodic LSV as a function of the total charge passed become noticeable after it has reached 1.4 Ah dm^{-3} (Fig. 2b). The shape of the LSV is rather similar to that shown in [9]. Three different regions can be distinguished. In the first region, from about −0.6 to −0.9 V, the current observed is very small. The second region presents a sharply rising wave starting at about −0.95 V. In this region deposition of CoPt alloy has been

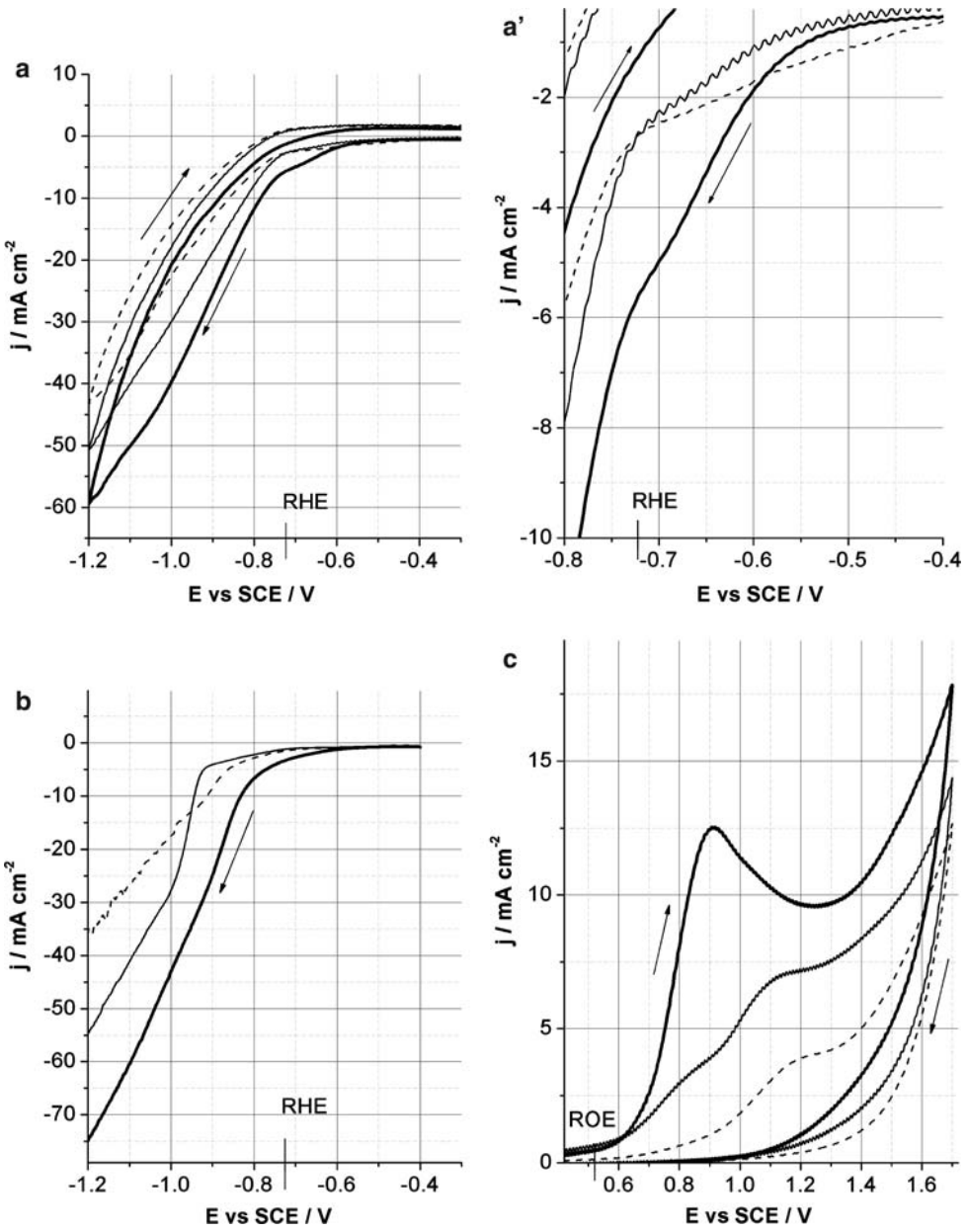

Fig. 2 Cathodic (**a**, **b**) and anodic voltammograms (**c**) for different total charges passed. Deposition in one-compartment cell from as-prepared electrolyte. (**a**, **a′** and **c**) cyclic voltammograms; (**a′**) inset in Fig. 2a; (**b**)—linear sweep voltammograms. The calculated potentials for hydrogen and oxygen evolution in the electrolytes used are −0.72 V and +0.51 V vs. SCE, respectively. ▬ 0.0 Ah dm^{-3}; — 1.4 Ah dm^{-3}, - - - 2.8 Ah dm^{-3}

observed. In the third region, −(1.0–1.2) V, the slopes are similar to those observed for as-prepared electrolyte, and are mainly associated with hydrogen evolution.

The CV in the anodic region exhibits a very strong dependence on total charge. The current density decreased with total charge and the peak at about +0.9 V totally disappeared when the total charge passed reached 2.8 Ah dm^{-3}. Additionally, a short plateau appears at 1.1–1.2 V. It should be noted that the effect of total charge passed is much more pronounced in the anodic than in the cathodic region. This is consistent with the observation that the electrochemical properties of the electrolyte are changed dramatically during anodic pre-oxidation, as will be shown below.

3.2.3 *Effect of total charge in two-compartment cells*

Operation of as-prepared electrolyte. When the total charge passed increased, the CV in the anodic and cathodic regions and cathodic LSV changed in the same way as observed for deposition in one-compartment cells (Fig. 3). However, the changes observed were slower in the two-compartment cells. For the CV in the cathodic region, the small wave starting at about −0.6 V disappeared only after 2.8 Ah dm^{-3}; polarization of the high wave reached about 0.1 V only after 4.2 Ah dm^{-3} (Fig. 3a). After 1.4 Ah dm^{-3}, the shape of cathodic LSV was still similar to that for as-prepared electrolyte (Figs. 2b and 3b), the peak at +0.9 V in the CV in the anodic region decreased to 8 mA cm^{-2}, as

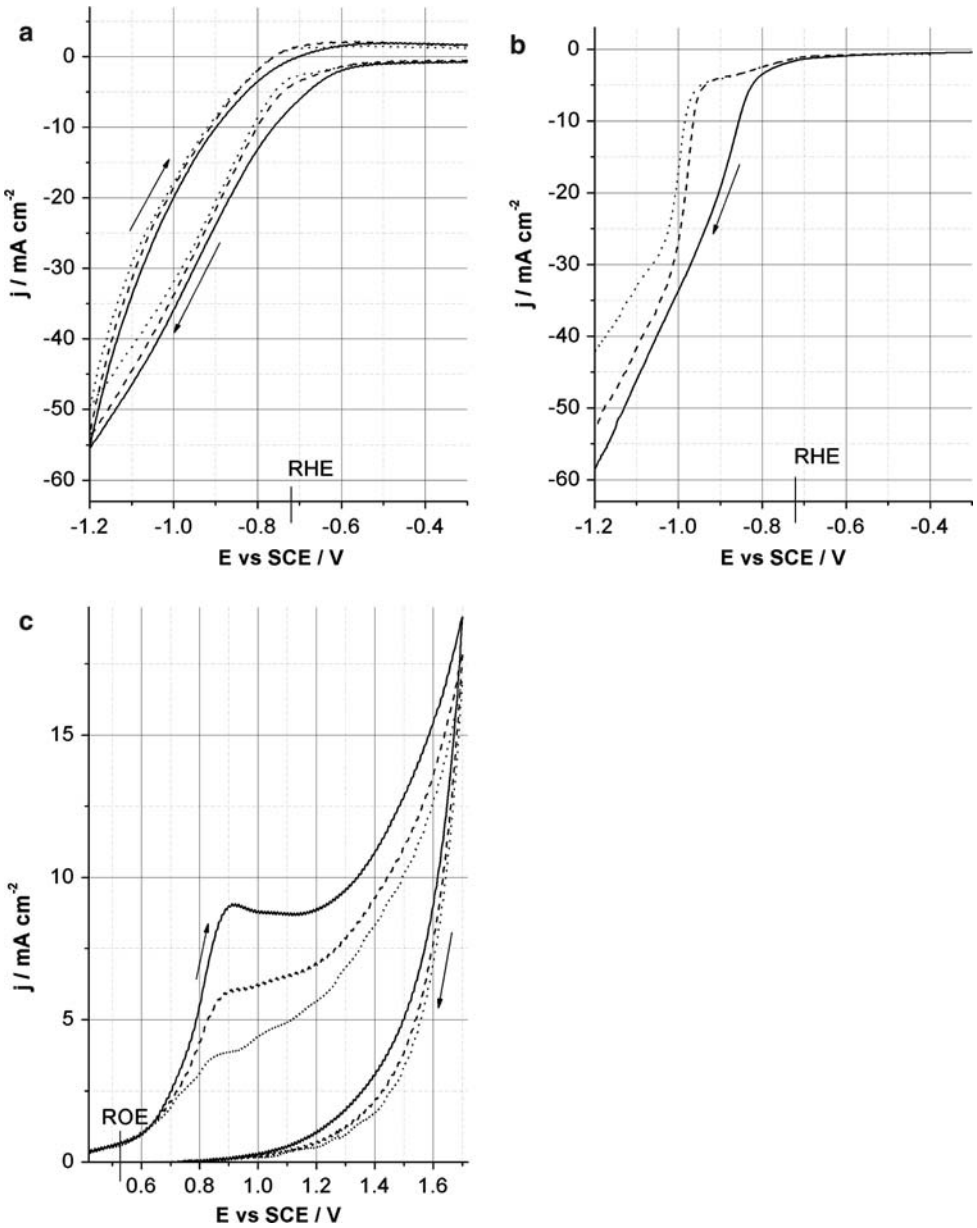

Fig. 3 Cathodic (**a**, **b**) and anodic voltammograms (**c**) for the different total charges passed. Deposition in two-compartment cell from as-prepared electrolyte. (**a**, **c**) cyclic voltammograms; (**b**) linear sweep voltammograms. — 1.4 Ah dm^{-3}, - - - 2.8 Ah dm^{-3}, ... 4.2 Ah dm^{-3}

seen in Fig. 3c, compared to 12.5 mA cm^{-2} in Fig. 2c for 0.0 Ah dm^{-3}.

Behavior of electrolyte pre-oxidized at the anode. The CV in the cathodic region, the cathodic LSV and the CV in the anodic region for the electrolyte pre-oxidized in the anodic compartment are shown in Fig. 4a–c, respectively. The results for electrolyte after pre-oxidation are designated as 0.0 Ah dm^{-3}. Anodic pre-oxidation changed the voltammograms in the same direction as the electrolyte operation in the one- or two-compartment cells (Figs. 2 and 3).

The increase in total charge up to 4.2 Ah dm^{-3} caused the same changes in the voltammograms (Fig. 4) as in operation of as-prepared electrolyte. In all cases, the increase in total charge passed in the deposition process, as well as the pre-oxidation of the electrolyte in the anode compartment, led to the following changes:

- Decrease in height of the small wave starting at −0.6 V and polarization of the high wave in the CV in the cathodic region;
- Decrease in current density, disappearance of the peak at +0.9 V and the appearance of an additional wave around +(1.1–1.2) V in the CV in the anodic region;
- Appearance of three regions in the LSV. The position and height of the characteristic wave in the second region changed with total charge passed.

The data indicate that both anodic and cathodic processes lead to changes in electrolyte composition, associated with

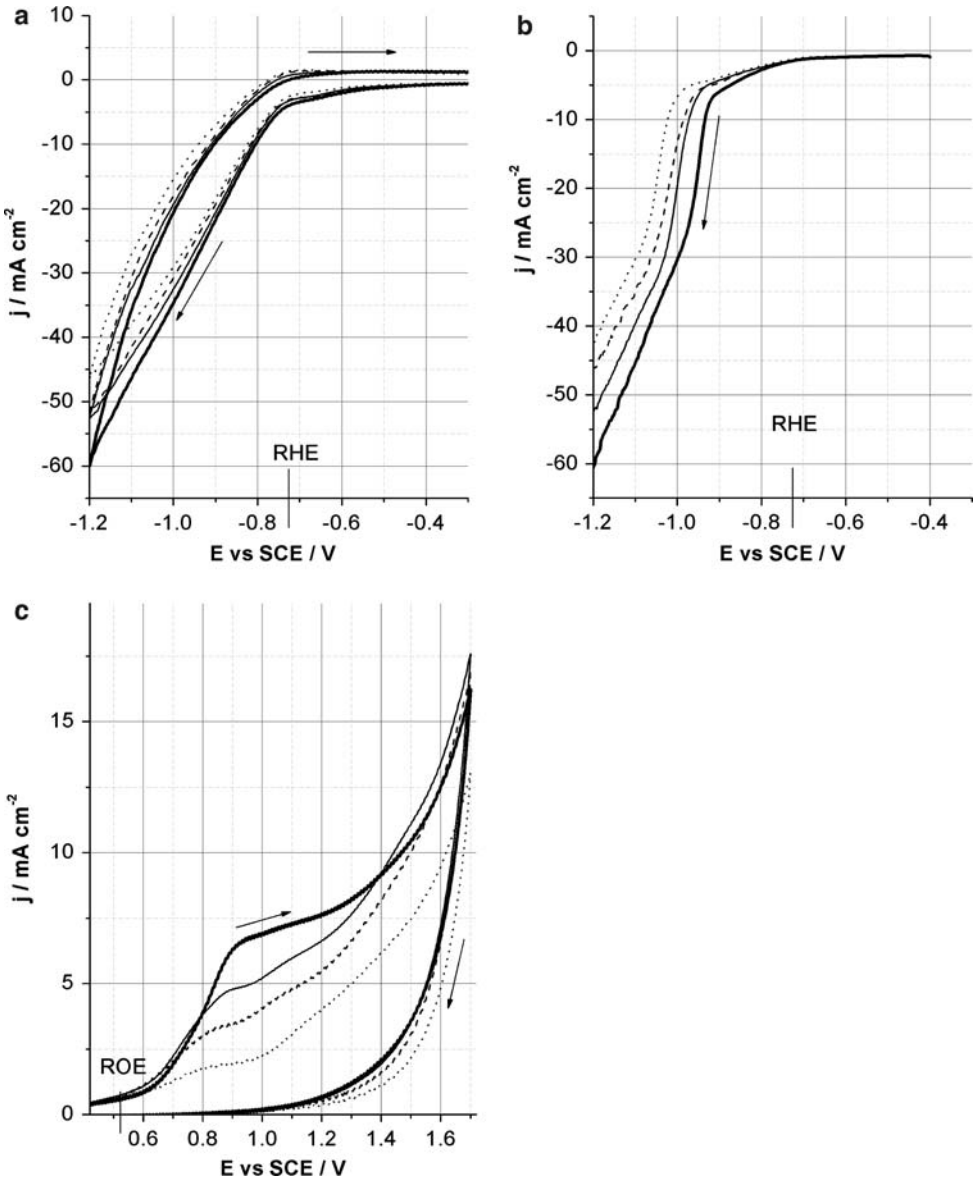

Fig. 4 Cathodic (**a**, **b**) and anodic voltammograms (**c**) for the different total charges passed. Deposition in two-compartment cell from electrolyte pre-oxidized at the anode. (**a**, **c**) cyclic voltammograms; (**b**) linear sweep voltammograms. ▬ 0.0 Ah dm^{-3}, —— 1.3 Ah dm^{-3}, - - - 2.7 Ah dm^{-3}, ... 4.2 Ah dm^{-3}

transformations of the Pt complex. The changes of the characteristics of the deposition process with total charge are associated with these transformations and are accompanied by an increase of CE.

3.3 Processes occurring during transformation of the Pt complex

In order to understand the anodic and cathodic processes occurring during transformation of the Pt-containing complex, we investigated voltammograms for solutions containing $[Pt(NO_2)_2\,(NH_3)_2]^0$ in comparison with solutions containing only the ligands in this complex, NO_2^- and NH_3.

Figure 5a shows CVs in the anodic region for 10 mM $[Pt(NO_2)_2(NH_3)_2]^0$ (solid line) and for 20 mM KNO_2, which yields the same concentration of NO_2^- (broken line). A solution of 0.1 M Na_2SO_4 served as the supporting electrolyte in both cases. The two voltammograms contain similar wide waves rising from +0.6 V with peaks near +0.9 V. The potentials of the peaks are in the range of the oxidation potentials of NO_2^- at Pt, +(0.80–0.95) V, reported for different experimental conditions [24, 30]. The oxidation peak for the solution containing the Pt complex is almost of the same height as that for the solution containing free NO_2^- (11.5 mA cm^{-2} vs. 10.7 mA cm^{-2}), indicating that it is due to the two-electron oxidation of NO_2^- to NO_3^- [24, 30]. The similarity of the waves unambiguously demonstrates that oxidation of NO_2^-, which is a part of the Pt complex, takes place. The NO_2^- anion is oxidized directly inside the complex and a fast equilibrium with the same species in solution does not have to be assumed, in agreement with existing literature [20–24]. The small shift

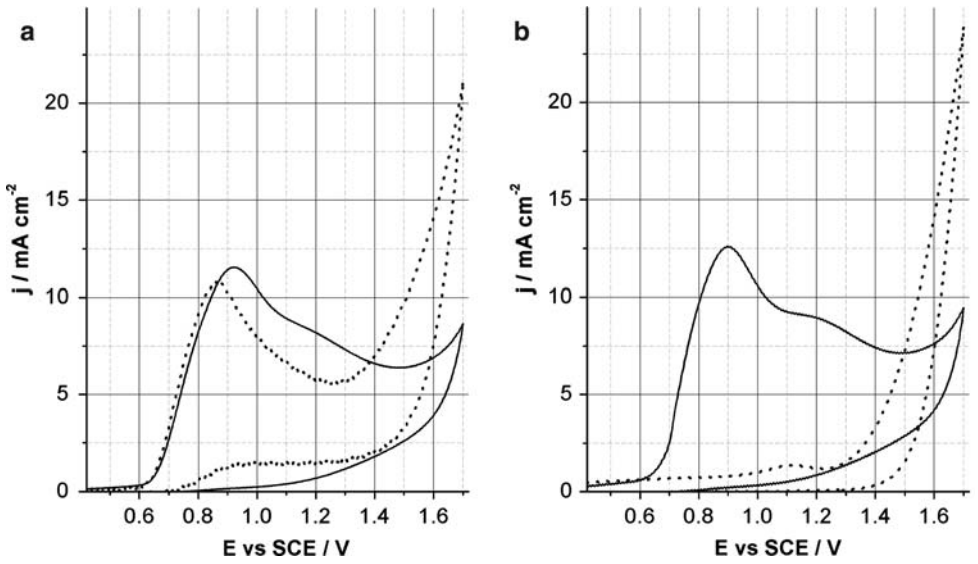

Fig. 5 Anodic cyclic voltammograms for $[Pt(NO_2)_2(NH_3)_2]^0$ complex compared to voltammograms for (**a**) KNO_2 and (**b**) $(NH_4)_2SO_4$ at pH 8. Sweep rate 100 mV s^{-1} (**a**) —— 10 mM Pt complex and 100 mM Na_2SO_4, - - - - 20 mM KNO_2 and 100 mM Na_2SO_4, (**b**) —— 10 mM Pt complex and 150 mM $(NH_4)_2SO_4$, - - - - 150 mM $(NH_4)_2SO_4$

in the peak potentials is indicative of the difference between oxidizing a free NO_2^- moiety in solution and the same species bound in the complex.

Changing the nature of one of the ligands in the complex (from NO_2^- to NO_3^-) changes its stability constant and this could explain the change of properties of a plating bath, which has been pre-oxidized at the anode, compared to an as-prepared electrolyte containing $[Pt(NO_2)_2(NH_3)_2]^0$.

The sharp rise in current starting at about +1.4 V is due to oxygen evolution (E_{rev} = +0.51 V vs. SCE). The rate of oxygen evolution is slower in the presence of the Pt complex, possibly because of its adsorption on the surface, blocking sites for intermediates involved in the electrochemical formation of molecular oxygen.

In Fig. 5b Na_2SO_4 has been replaced by $(NH_4)_2SO_4$. This has little effect on the shape of the curve in the presence of $[Pt(NO_2)_2(NH_3)_2]^0$ (solid line) but in the absence of NO_2^- in the system (dotted line) the peak at +0.9 V, SCE disappears. This peak can therefore be definitely associated with oxidation of NO_2^-, whether it is part of the complex or free in solution. In the voltammogram for $(NH_4)_2SO_4$ (dotted line), a small wave with a peak of about 1.35 mA cm^{-2} at +1.1 V is observed. The oxidation of ammonia in this potential region may account for the higher values of the oxidation current for the Pt complex compared to that for NO_2^- in the range of potentials of +(0.8–1.4 V), as well as to the shift of oxidation potentials (Fig. 5a). The suggestion that oxidation of both NO_2^- and NH_3 occurs is consistent with the presence of two waves in the CVs in the anodic region for the electrolytes after electrolysis (Figs. 2–4).

The CVs in the cathodic regions for 20 mM KNO_2 both in Na_2SO_4 and Na_3Cit as the supporting electrolytes contain a small wave rising from −0.6 V with peaks at −(0.8–0.83) V and heights of about 2 mA cm^{-2}, as shown in Figs. 6 and 7. These peaks shift to about −0.7 V in the presence of $(NH_4)_2SO_4$. Addition of 20 mM $(NH_4)_2SO_4$ to the electrolyte results in the appearance of a wave rising at −0.75 V and tending to form a plateau at −(0.9–0.95) V. The height of this wave increases with the concentration of NH_4^+, as seen in Fig. 7, but no significant increase of the small wave rising at −0.6 V, associated with NO_2^- reduction, is observed.

The CVs for Pt complex (10 mM) are very close to those for KNO_2 (20 mM) in {0.1 M Na_2SO_4 + 20 mM $(NH_4)_2SO_4$} and {0.1 M Na_3Cit + 20 mM $(NH_4)_2SO_4$} supporting electrolytes, as seen in Fig. 6. In voltammograms for Pt complex in Na_2SO_4 (Fig. 6b), a small wave in the potential range of −(0.6–0.8) V is barely noticeable, while in the case of citrate supporting electrolyte it is seen rather clearly (Figs. 6a). The wave rising at −0.6 V is also observed in the CV for as-prepared citrate electrolyte (Fig. 2a). This indicates that there is some interaction between the Pt complex and the citrate, possibly with some degree of substitution of NO_2^- in the complex. An ion of NO_2^- removed from the Pt complex can be reduced at the cathode. The reduction of the same ion, while it is bound as a ligand in the complex, seems to be inhibited, while there is only a small difference in the oxidation of bound and free NO_2^-. Enhancement of cathodic reduction of free NO_2^- by high-temperature hydrolysis of $[Pt(NO_2)_4]^{2-}$ was reported by Pletcher et al. [24].

In the CV in the cathodic region for as-prepared electrolyte, the small wave rising at −0.6 V disappears after deposition in a two-compartment cell, where the anolyte and catholyte are essentially isolated from each other (Fig. 3a). In the CV in the anodic region, after operation in two-compartment cells, the peak at +0.9 V, associated with the oxidation of NO_2^- also decreases and disappears with increasing total charge (Fig. 3c), indicating the decrease of

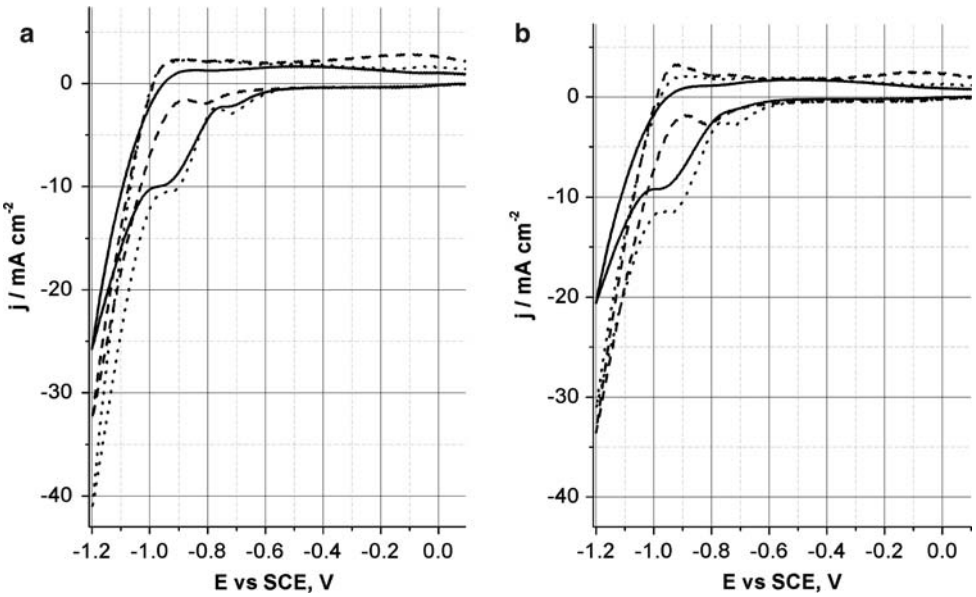

Fig. 6 Cathodic cyclic voltammograms $[Pt(NO_2)_2(NH_3)_2]^0$ complex compared to voltammograms for KNO_2 and simultaneously presented KNO_2 and $(NH_4)_2SO_4$ at pH 8. Sweep rate 100 mV s^{-1} (**a**) Background: 100 mM Na_3 Cit —— 10 mM Pt complex, - - - - - 20 mM KNO_2, ... 2 mM KNO_2 + 20 mM $(NH_4)_2SO_4$; (**b**) Background: 100 mM Na_2SO_4 —— 10 mM Pt complex, - - - - - 20 mM KNO_2, ... 2 mM KNO_2 + 20 mM $(NH_4)_2SO_4$

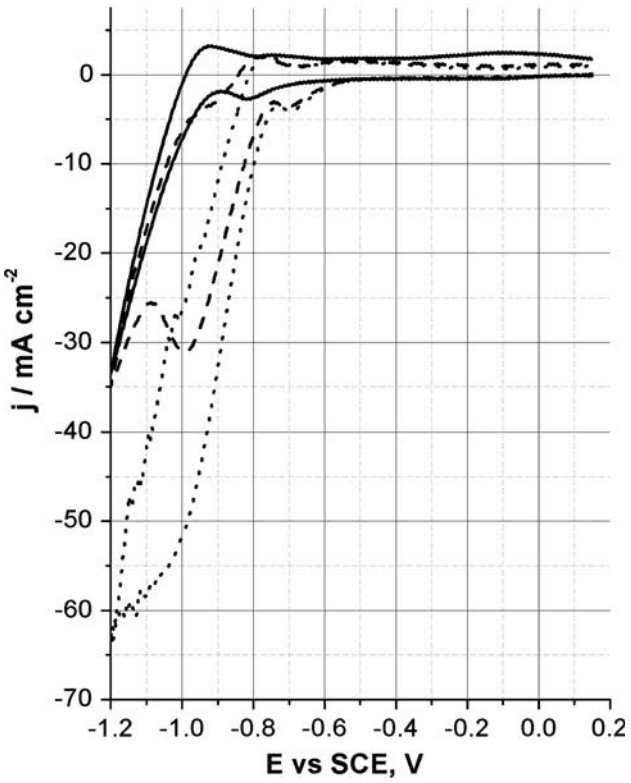

Fig. 7 Cathodic voltammograms for KNO_2 in different background electrolytes at pH 8. Sweep rate 100 mV s^{-1} —— 100 mM Na_2SO_4, - - - - 100 mM Na_2SO_4, 70 mM $(NH_4)_2SO_4$, ... 100 mM Na_2SO_4, 150 mM $(NH_4)_2SO_4$

NO_2^- concentration. These observations show that the reduction of NO_2^- occurs during CoPt deposition. It should be noted that the possibility of NO_2^- reduction during Pt deposition from nitrite-aqua-complex to NH_4^+ has already been discussed in the literature [24, 27].

The wave starting at about −0.75 V and increasing with ammonium concentration can be associated with hydrogen evolution, with the ammonium ion serving as the source of protons

$$2NH_4^+ + 2e^- \rightarrow H_2 + 2NH_3 \quad (1)$$

Although during electrolysis, removal of NH_3 can occur as a result of evaporation, the decreases of the wave under discussion with total charge can also be associated with reduction of ammonium ion during deposition, as shown in Eq. 1 (cf. Figs. 2–4).

In alkaline (pH 10–10.5) and acid (pH 0–2) electrolytes, $[Pt(NH_3)_{4-x}(H_2O)_x]^{2+}$ and $[PtCl_{4-x}(H_2O)_x]^{2-x}$, respectively, were formed [20–22]. Electroplating of Pt occurs in such solutions by ligand displacement, followed by reduction of $[Pt(H_2O)_4]^{2+}$. Substitution of ligands (especially NH_3) proceeds extremely slowly and does not occur significantly on the time-scale of voltammetric experiments, even at 95 °C. The complex $[Pt(H_2O)_4]^{2+}$ is stable only in highly acidic media. In the baths containing Pt complexes with ammonia, it was postulated that the electrode can catalyze the ligand-substitution reaction, forming $[Pt(H_2O)_4]^{2+}$, which is consumed immediately by reduction to metallic platinum. This is consistent with the fact that Pt deposition from alkaline electrolyte occurs only at temperatures close to the boiling point, where NH_3 is substituted by H_2O as the ligand.

The results of the present work indicate that formation of new electroactive Pt-containing complexes may result from transformation of $[Pt(NO_2)_2(NH_3)_2]^0$ on both the cathode and the anode. The exact nature of the electroactive species formed as a result of electrolysis has not yet been identified. However, it seems to be stable, since long-term storage of the electrolyzed solutions does not cause any change of the CE for deposition of the CoPt alloy.

4 Conclusions

The total-charge effect during deposition of CoPt alloys in one- and two-compartment cells from the as-prepared electrolyte containing $[Pt(NO_2)_2(NH_3)_2]^0$ and from the electrolyte pre-oxidized in the anode compartment was studied. Monitoring the electrolyte during operation by means of cyclic and LSV in anodic and cathodic potential regions showed the impact of total charge on the nature of the Pt complex and on the characteristics of the deposition process. The total charge effect is associated with transformations of Pt complex during electrolysis, as indicated by voltammetry. New electroactive Pt-containing complexes result from transformation of $[Pt(NO_2)_2(NH_3)_2]^0$ on both the cathode and the anode. It was found that, at the anode, the main reactions were oxidation of NO_2^-, and to a lesser extent of NH_3, while at the cathode the main reactions were the reduction of NO_2^- in addition to deposition of the alloy and hydrogen evolution.

Using anodic pretreatment of solutions containing the Pt complex as part of the preparation of an electrolyte was found to stabilize the process significantly. However, the optimization of the procedure for electrolyte preparation is beyond the scope of the present work.

Acknowledgements This work was partially supported by the Office of the Chief Scientist, Israel Ministry of Trade and Industry. One of us (O. B.) wishes to thank the "KAMEA" program of the Israeli Ministry of Absorption for support in the course of this project

References

1. Chin Ts-Sh (2000) J Magn Magn Mater 209:75
2. Myung NV, Park D-Y, Yoo B-Y, Sumodjo PTA (2003) J Magn Magn Mater 265:189
3. Xiao QF, Bruck E, Zhang ZD, de Boer FR, Buschow KHJ (2002) J Appl Phys 91:304
4. Fujita N, Maeda S, Yoshida S, Takase M, Nakano M, Fukunaga H (2004) J Magn Magn Mater 272–276:e1895
5. Wang F, Hosoiri K, Doi S, Okamoto N, Kuzushima T, Totsuka T, Watanabe T (2004) Electrochem Commun 6:1149
6. Bozzini B, De Vita D, Sportoletti A, Zangari G, Cavallotti PL, Terrenzio E (1993) J Magn Magn Mater 120:300
7. Callegaro L, Puppin E, Cavallotti PL, Zangari G (1996) J Magn Magn Mater 155:190
8. Zangari G, Bucher P, Lecis N, Cavallotti PL, Callegaro L, Puppin E (1996) J Magn Magn Mater 157/158:256
9. Cavallotti PL, Lecis N, Fauser H, Zielonka A, Celis JP, Wouters G, Machado da Silva J, Brochado Oliveira JM, Sa MA (1998) Surf Coat Technol 105:232
10. Zana Iu, Zangari G (2003) Electrochem Solid-state Lett 6(12):C153
11. Zana Iu, Zangari G (2004) J Magn Magn Mater 272–276:1698
12. Franz S, Cavallotti PL, Bestetti M, Sirtori V, Lombardi L (2004) J Magn Magn Mater 272–276:2430
13. Zana Iu, Zangari G, Shamsuzzoha M (2004) J Electrochem Soc 151(10):C637
14. Ghidini M, Zangari G, Prejbeanu IL, Pattanaik G, Buda-Prejbeanu LD, Asti G, Pernechele C, Solzi M (2006) J Appl Phys 100:103911
15. Pattanaik G, Kirkwood DM, Xu X, Zangari G (2007) Electrochim Acta 52:2755
16. Xu X, Weston J, Zangari G (2007) J Appl Phys 101:09K520
17. Eagleton TS, Mallet J, Cheng X, Wang J, Chien C-L, Season PC (2005) J Appl Phys 152(1):C27
18. Kulkarni S, Roy S (2007) J Appl Phys 101:09K524
19. Berkh O, Rosenberg Yu, Shacham-Diamand Y, Gileadi E (2007) Microelectron Eng 84:2444
20. Le Penven R, Levason W, Pletcher D (1992) J Appl Electrochem 22:415
21. Gregory AJ, Levason W, Pletcher D (1993) J Electroanal Chem 348:211
22. Gregory AJ, Levason W, Noftle RE, Penven RLe, Pletcher D (1995) J Electroanal Chem 399:105
23. Basirun WJ, Pletcher D, Saraby-Reintjes A (1996) J Appl Electrochem 26:873
24. Levason W, Pletcher D, Smith AM, Berzins AR (1998) J Appl Electrochem 28:18
25. Baumgarten ME, Raub ChJ (1988) Platinum Met Rev 32:188
26. Skinner BE (1989) Platinum Met Rev 33:102
27. Pushpavanam M (2006) J Appl Electrochem 36:1069
28. Rao CRK, Trivedi DC (2005) Coord Chem Rev 249:613
29. Donten M, Osteryoung J (1991) J Appl Electrochem 21:496
30. Cortona MN, Vettorazzi NR, Silber JJ, Serano LE (1999) J Electroanal Chem 470:157